Design of Robust UPFC Controller Using H∞ Control Theory in Electric Power System

Seyed Abbas Taher, Shahabeddin Akbari,Ali Abdolalipour and Reza Hematti
Department of Electrical Engineering,
University of Kashan, Kashan, Iran

Abstract: An industrial plant, such a power system, always contains parametric uncertainties. In the design of a controller the uncertainties have to be considered. Otherwise, if the real plant differs from the assumed plant model, a controller, designed based on classical controller design approaches, may not ensure the stability of the overall system. In this paper design of robust control for the UPFC controllers including power - flow and DC voltage regulator, using a H_∞ loop-shaping design via a normalized coprime factorization approach, where loop-shape refers to magnitude of the loop transfer function $L = GK$ as function of frequency is presented. As an example, we have designed a case for the system to compare the proposed method with a conventional method (classical P-I controller). AS the results of the linear and nonlinear simulations, the validity of the proposed method has been confirmed.

Key words: Unified Power Flow Controller (UPFC); Flexible AC Transmission Systems (FACTS); power system oscillation; H_∞ loop-shaping

INTRODUCTION

The Flexible AC Transmission Systems (FACTS) based on power electronics offer an opportunity to enhance controllability, stability, and power transfer capability of AC transmission systems[1]. The Unified Power Flow Controller (UPFC), which is the most versatile FACTS device, has the capabilities of controlling power flow in the transmission line, improving the transient stability, mitigating system oscillation and providing voltage support[2-4]. PID is the most commonly used control algorithm in the process industry. Also, this technique is used to control the FACTS devices[5]. However, the nonlinear nature of well as the uncertainties that exist in the system make it difficult to design an effective controller for the FACTS that guarantees fast and stable regulation under all operating conditions. A major source of difficulty is that open-loop plant may change. In particular, inaccuracy in plant may cause problems because the plant is part of the feedback loop. To deal with such a problem, instead of using a single model plant, an uncertain model should be considered. This problem has led to the study of applying adaptive controllers for instance[6, 7], nonlinear controllers for instance[8] in the power system stability control. Also, during past decade, the H_∞ optimal robust control design has received increasing attention in power systems. Most of above methods have been applied in power systems and some of these efforts have contributed to the design of supplementary control for SVC using mixed sensitivity[9], applying μ-synthesis for SVC in order to voltage control design[10] and supplementary control design for SVC and STATCOM[11]. For many control problems, a design procedure is required that offers more flexibility than mixed sensitivity, but should not be as complicated as μ-synthesis and should not be limited in its application like LTR procedures. The H_∞ loop-shaping design is such a controller procedure, used to design a robust controller for FACTS control to improve the system damping[12].

In this paper as an example, a Single Machine Infinite Bus (SMIB) power system installed with a UPFC is considered for case study and H_∞ loop-shaping method is used to design a robust controller for UPFC controller including power-flow and DC-voltage regulator in this system. To show influence of proposed method, the proposed method is compared to conventional method (the parameters of conventional P-I controller are optimized using genetic algorithm). As the validity of the proposed method has been confirmed by linear and nonlinear time domain simulation results.

MATRIALS AND METHODS

Figure 1 shows a SMIB system equipped with a UPFC. The UPFC consists of an Excitation Transformer (ET), a Boosting Transformer (BT), two three-phase GTO based voltage source converters
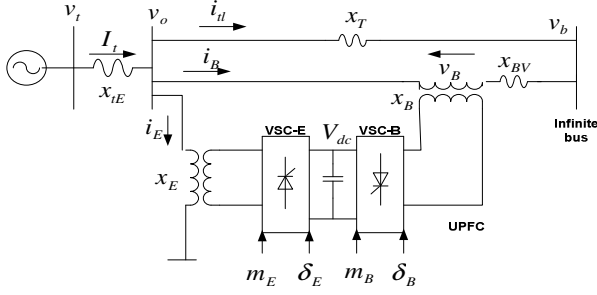
Corresponding Author: Seyed Abbas Taher, Depatment of Electrical Engineering, University of Kashan, Kashan, Iran

Fig. 1: SMIB power system equipped with UPFC

(VSCs) and a DC link capacitors. The four input control signals to the UPFC are m_E, m_B, δ_E, and δ_B, where, m_E is the excitation amplitude modulation ratio, m_B is the boosting amplitude modulation ratio, δ_E is the excitation phase angle and δ_B is the boosting phase angle.

Non-Linear Dynamic Model: By applying Park's transformation and neglecting the resistance and transients of the ET and BT transformers, the UPFC can be modeled as[13-15]:

$$\begin{bmatrix} v_{Etd} \\ v_{Etq} \end{bmatrix} = \begin{bmatrix} 0 & -x_E \\ x_E & 0 \end{bmatrix}\begin{bmatrix} i_{Ed} \\ i_{Eq} \end{bmatrix} + \begin{bmatrix} \dfrac{m_E \cos\delta_E v_{dc}}{2} \\ \dfrac{m_E \sin\delta_E v_{dc}}{2} \end{bmatrix} \qquad (1)$$

$$\begin{bmatrix} v_{Btd} \\ v_{Btq} \end{bmatrix} = \begin{bmatrix} 0 & -x_B \\ x_B & 0 \end{bmatrix}\begin{bmatrix} i_{Bd} \\ i_{Bq} \end{bmatrix} + \begin{bmatrix} \dfrac{m_B \cos\delta_B v_{dc}}{2} \\ \dfrac{m_B \sin\delta_B v_{dc}}{2} \end{bmatrix} \qquad (2)$$

$$\dot{v}_{dc} = \frac{3m_E}{4C_{dc}}[\cos\delta_E \quad \sin\delta_E]\begin{bmatrix} i_{Ed} \\ i_{Eq} \end{bmatrix}$$
$$+ \frac{3m_B}{4C_{dc}}[\cos\delta_B \quad \sin\delta_B]\begin{bmatrix} i_{Bd} \\ i_{Bq} \end{bmatrix} \qquad (3)$$

Where, v_{ET}, i_E, V_{Bt} and i_B are the excitation voltage, excitation current, boosting voltage, and boosting current, respectively; c_{dc} and v_{dc} are the DC link capacitance and voltage, respectively. The nonlinear model of the SMIB system as shown in Fig. 1 is described by:

$$\dot{\omega} = (P_m - P_e - D\Delta\omega)/M \qquad (4)$$

$$\dot{\delta} = \omega_0(1 - \omega) \qquad (5)$$

$$\dot{E}'_q = (-E_q + E_{fd})/T'_{do} \qquad (6)$$

$$\dot{E}_{fd} = (-E_{fd} + K_a(V_{ref} - V_t))/T_a \qquad (7)$$

Where,

$$P_e = V_{td}I_{td} + V_{tq}I_{tq}; E_q = E'_{qe} + (X_d - X'_d)I_{td}$$

$$V_t = V_{td} + jV_{tq}; V_{td} = X_q I_{tq}; V_{tq} = E'_q - X'_d I_{td}$$

$$I_{td} = I_{tld} + I_{Ed} + I_{Bd}; I_{tq} = I_{tlq} + I_{Eq} + I_{Bq}$$

$$I_{tld} = \frac{x_E}{X_T}I_{Ed} + \frac{1}{X_T}\frac{m_e V_{dc}}{2}\cos\delta_E - \frac{1}{X_T}V_b\cos\delta$$

$$I_{tlq} = \frac{x_E}{X_T}I_{Eq} - \frac{1}{X_T}\frac{m_e V_{dc}}{2}\sin\delta_E + \frac{1}{X_T}V_b\sin\delta$$

$$I_{Ed} = \frac{(x_{dt} - x_{BB}x_{b3})}{x_{dE}}V_b\cos\delta - \frac{x_{dt}}{x_{dE}}\frac{m_B V_{dc}}{2}\cos\delta_B$$
$$+ \frac{x_{BB}}{x_{dE}}E' - \frac{(x_{dt} + x_{BB}x_{b2})}{x_{dE}}\frac{m_e V_{dc}}{2}\cos\delta_E$$

$$I_{Eq} = \frac{(x_{dt} + x_{BB}x_{a3})}{x_{qE}}V_b\sin\delta - \frac{x_{qt}}{x_{qE}}\frac{m_B V_{dc}}{2}\sin\delta_B$$
$$- \frac{(x_{qt} + x_{BB}x_{a2})}{x_{qE}}\frac{m_e V_{dc}}{2}\sin\delta_E$$

$$I_{Bd} = \frac{(x_{b3}x_E - x_{b1})}{x_{dE}}V_b\cos\delta + \frac{x_{b1}}{x_{dE}}\frac{m_B V_{dc}}{2}\cos\delta_B$$
$$+ \frac{x_E}{x_{dE}}E'_q + \frac{x_{b1} - x_E x_{b2}}{x_{dE}}\frac{m_e V_{dc}}{2}\cos\delta_E$$

$$I_{Bq} = -\frac{(x_{a3}x_E + x_{b1})}{x_{qE}}V_b\sin\delta + \frac{x_{a1}}{x_{qE}}\frac{m_B V_{dc}}{2}\sin\delta_B$$
$$+ \frac{(x_{a1} - x_E x_{a2})}{x_{qE}}\frac{m_e V_{dc}}{2}\sin\delta_E$$

$$x_{dT} = X_{tE} + X'_d; \quad x_{qT} = X_q + X_{tE}; \quad x_{ds}$$
$$= X_E + x_{dT}; \quad x_{qs} = X_E + x_{qT}$$

$$x_{a1} = \frac{(x_{qs}X_T + x_{qT}X_E)}{X_T}; \quad x_{a2} = 1 + \frac{x_{qT}}{X_T}; \quad x_{a3} = -\frac{x_{qT}}{X_T};$$

$$x_{b1} = \frac{(x_{ds}X_T + x_{dT}X_E)}{X_T}; \quad x_{b2} = 1 + \frac{x_{dT}}{X_T}; \quad x_{b3} = \frac{x_{dT}}{X_T}$$

$$x_{dE} = (\frac{x_{BB}x_{dT}X_E}{X_T} + x_E x_{dT} + x_{BB}x_{ds}); \quad x_{qE}$$
$$= -(\frac{x_{BB}x_{qT}X_E}{X_T} + x_E x_{qT} + x_{BB}x_{qs})$$

The equation for real power balance between the series and shunt converters is given by:

$$\text{Re}(V_B I_B^* - V_E I_E^*) = 0 \qquad (8)$$

Power system linearised model: A linear dynamic model is obtained by linearising the nonlinear model round an operating condition. The linearised model of power system as shown in Fig. 1 is given as follows:

$$\Delta \dot{\delta} = \omega_0 \Delta \omega \qquad (9)$$

$$\Delta \dot{\omega} = (-\Delta P_e - D\Delta \omega)/M \qquad (10)$$

$$\Delta \dot{E}_q^{/} = (-\Delta E_q + \Delta E_{fd})/T_{do}^{/} \qquad (11)$$

$$\Delta \dot{E}_{fd} = -\frac{1}{T_A}\Delta E_{fd} - \frac{K_A}{T_A}\Delta V \qquad (12)$$

$$\Delta \dot{v}_{dc} = K_7\Delta\delta + K_8\Delta E_q^{/} - K_9\Delta v_{dc} + K_{ce}\Delta m_E \\ + K_{c\delta e}\Delta\delta_E + K_{cb}\Delta m_B + K_{c\delta b}\Delta\delta_B \qquad (13)$$

Where,

$$\Delta P_e = K_1\Delta\delta + K_2\Delta E_q^{/} + K_{pd}\Delta v_{dc} + K_{pe}\Delta m_E \\ + K_{p\delta e}\Delta\delta_E + K_{pb}\Delta m_B + K_{p\delta b}\Delta\delta_B$$

$$\Delta V_t = K_5\Delta\delta + K_6\Delta E_q^{/} + K_{vd}\Delta v_{dc} + K_{ve}\Delta m_E \\ + K_{v\delta e}\Delta\delta_E + K_{vb}\Delta m_B + K_{v\delta b}\Delta\delta_B$$

$$\Delta E_q^{/} = K_4\Delta\delta + K_3\Delta E_q^{/} + K_{qd}\Delta v_{dc} + K_{qe}\Delta m_E \\ + K_{q\delta e}\Delta\delta_E + K_{qb}\Delta m_B + K_{q\delta b}\Delta\delta_B$$

K_1, K_2…K_9, K_{pu} ,K_{qu} and K_{vu} are linearization constants. The state-space model of power system is given by:

$$\dot{x} = Ax + Bu \qquad (14)$$

Where, the state vector x, control vector u, A and B are:

$$x = [\Delta\delta \quad \Delta\omega \quad \Delta E_q^{/} \quad \Delta E_{fd} \quad \Delta v_{dc}]$$
$$u = [\Delta m_E \quad \Delta\delta_E \quad \Delta m_B \quad \Delta\delta_B]^T$$

The block diagram of the linearised dynamic model of the SMIB power system with UPFC is shown in Fig. 2.

H_∞ Loop-shaping design: The adopted control method is based on H_∞ robust stabilization combined with classical Loop-shaping, where loop-shape refers to the magnitude of the loop transfer function L = GK as a function of frequency. It is essentially a tow-step procedure, where in the first step; the singular values of the open-loop plant are shaped by pre and post compensators. In the second step, the resulting shaped plant is robustly stabilized with respect to coprime factor uncertainty using H_∞ optimization. An important advantage is that no problem-dependent uncertainty modeling, or weight selection, is required in this second step[16].

The stabilization of a plant G is considered, that has a normalized left coprime factorization as follows[16]:
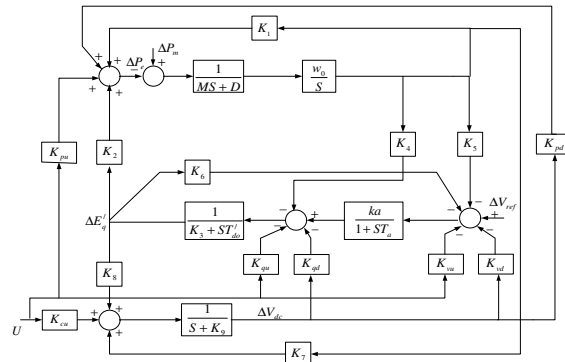

Fig. 2: linearised dynamic model of the SMIB power system with UPFC

$$A = \begin{bmatrix} 0 & w_0 & 0 & 0 & 0 \\ -\dfrac{K_1}{M} & 0 & -\dfrac{K_2}{M} & 0 & -\dfrac{K_{pd}}{M} \\ -\dfrac{K_4}{T_{do}^{/}} & 0 & -\dfrac{K_3}{T_{do}^{/}} & \dfrac{1}{T_{do}^{/}} & -\dfrac{K_{qd}}{T_{do}^{/}} \\ -\dfrac{K_A K_5}{T_A} & 0 & -\dfrac{K_A K_6}{T_A} & -\dfrac{1}{T_A} & -\dfrac{K_A K_{vd}}{T_A} \\ K_7 & 0 & K_8 & 0 & -K_9 \end{bmatrix}$$

$$B = \begin{bmatrix} 0 & 0 & 0 & 0 \\ -\dfrac{K_{pe}}{M} & -\dfrac{K_{p\delta e}}{M} & -\dfrac{K_{pb}}{M} & -\dfrac{K_{p\delta b}}{M} \\ -\dfrac{K_{qe}}{T_{do}^{/}} & -\dfrac{K_{q\delta e}}{T_{do}^{/}} & -\dfrac{K_{qb}}{T_{do}^{/}} & -\dfrac{K_{q\delta b}}{T_{do}^{/}} \\ -\dfrac{K_A K_{vc}}{T_A} & -\dfrac{K_A K_{v\delta e}}{T_A} & -\dfrac{K_A K_{vb}}{T_A} & -\dfrac{K_A K_{v\delta b}}{T_A} \\ K_{ce} & K_{c\delta e} & K_{cb} & K_{c\delta b} \end{bmatrix}$$

That has a normalized left coprime factorization as follows:

$$G = M^{-1} \qquad (15)$$

A perturbed plant model G_d can then be written as:

$$G_p = (M + \Delta_M)^{-1} + (N + \Delta_N) \qquad (16)$$

Where Δ_M and Δ_N represent the uncertainty in the nominal plant model G. The objective of robust stabilization is to stabilize a family of perturbed plants defined by:

$$G_p = \left\{ (M + \Delta_M)^{-1} + (N + \Delta_N) : \left\| \begin{matrix} \Delta_N & \Delta_M \end{matrix} \right\|_\infty \prec \varepsilon \right\} \qquad (17)$$

Where $\varepsilon > 0$ is then the stability margin. For the perturbed feedback system of Fig. 3, the stability
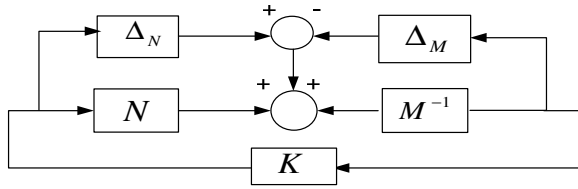
Fig. 3: H$_\infty$ robust stabilization problem

Fig. 4: shaped plant and controller

property is Robust if and only if, the nominal feedback system is stable and:

$$\gamma \overset{\Delta}{=} \left\| \begin{bmatrix} K \\ I \end{bmatrix} (I - GK)^{-1} M^{-1} \right\|_\infty \leq \frac{1}{\varepsilon} \qquad (18)$$

The lowest achievable value of y and corresponding maximum stability margin ε are given by:

$$\gamma_{\min} = \varepsilon_{MAX}^{-1} = \{1 - \| \begin{bmatrix} N & M \end{bmatrix} \|_H^Z \}^{1/2} = (1 + \rho(X_z))^{1/2} \qquad (19)$$

Where $\|.\|_H$ denotes the Hankel norm, p denotes radius (maximum eigenvalue), and for a minimal stat space realization (A, B, C, D) of G, Z and X are the unique positive definite solution to the algebraic Riccati equations:

$$Z : \left(A - BS^{-1}D^TC \right) Z + Z \left(A - BS^{-1}D^TC \right)^T$$
$$- ZC^TR^{-1}CZ + BS^{-1}B^T = 0 \qquad (20)$$

$$X : \left(A - BS^{-1}D^TC \right) X + X \left(A - BS^{-1}D^TC \right)$$
$$- XBS^{-1}B^TX + C^TR^{-1}C = 0 \qquad (21)$$

Where $R = I + DD^T$ and $S = I + D^TD$.
A controller, which guarantees that

$$\left\| \begin{bmatrix} K \\ I \end{bmatrix} (I - GK)^{-1} M^{-1} \right\|_\infty \leq \gamma$$

For a specified y > y is given by:

$$K \overset{\Delta}{=} \begin{bmatrix} A + BF + \gamma^2 \left(L^T \right)^{-1} ZC^T (C + DF) & \gamma^2 \left(L^T \right)^{-1} ZC^T \\ B^TX & -D^T \end{bmatrix} \qquad (22)$$

Where $F = -S^{-1} \left(D^TC + B^TX \right)$ and $L = (1 - \gamma^2)I + ZX$.

It is important to emphasizes that, since $y_{\min}$ is computed from (19) and an explicit solution has been derived by solving just two Riccati equations and the y iteration needed to solve them, the general H$_\infty$ problem has been avoided[16-17].
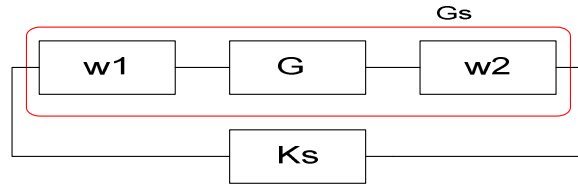
The controller design procedure can be summarized as follows.

Loop Shaping: Using pre- and post compensators W1 and W2, the singular values of the plant are shaped to give a desired open loop shape as shown in Fig. 4. Some trial and error is involved Here W2 is usually chosen as a constant. W1 contains dynamic shaping. Integral action for low frequency performance, phase-advance for reducing the roll-off rates at crossover, and phase-lag to increase the roll-off rates at high frequencies, should all be placed in W1 if desired. The weights should be chosen so that no unstable hidden modes are created in G$_s$.

Robust Stabilization: Robustly stabilize the shaped plant G$_s$. First, calculate the maximum stability margin $\varepsilon_{max} < 1/y_{min}$. If the margin is too small, $\varepsilon_{max} < 0.25$, return to step 1 and adjust the weight. Otherwise, select $y > y_{min}$ by about 10% and synthesis a suboptimal controller using (22). When $\varepsilon_{max} > 0.25$ (respectively, $y_{min} < 4$) the design is usually successful. A small value of ε_{max} indicates that the chosen singular value loop shapes are incompatible with robust stability requirements. The loop shape does not change much following robust stabilization if y is small[16-17].

If all the specification is not met: Return to step 1 and make further modification to the weights.

Reduce the order of controller: Check the frequency response plot of K$_{s-red}$ against that of K$_s$.

Final feedback controller K: This is achieved by combining K$_{s-red}$ with the shaping function W1 and W2 such that $K = W1 K_{s-red} W2$.

UPFC CONTROLLERS

The UPFC control system comprises following controllers:
- Power flow controller
- DC voltage regulator controller
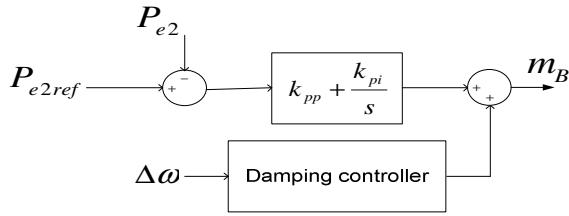- Power system oscillation-damping controller

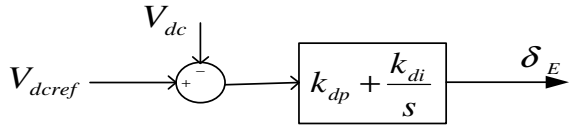Fig. 5: Power flow controller with damping controller

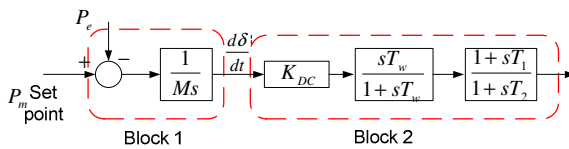
Fig. 6: DC voltage regulator

Fig. 7: Transfer function block diagram of the UPFC based damping controller

Power flow and DC voltage regulator controllers: The UPFC is installed in one of the two lines of the SMIB system. Figure 5 shows the transfer function of the power flow controller. The power flow controller regulates the power flow on this line. k_{pp} and k_{pi} are the proportional and integral gain of the power flow controller. The real power output of the shunt converter must be equal to the real power input of the series converter or vice versa. In order to maintain the power balance between the two converters, a DC-voltage regulator is incorporated. DC-voltage is regulated by modulating the phase angle of the shunt converter voltage. A P-I type DC-voltage regulator is considered Fig. 6. k_{dp} and k_{di} are the proportional and integral gain of the DC-voltage regulator.

Power system oscillation-damping controller: A damping controller is provided to improve the damping of power system oscillations. This controller may be considered as a lead-lag compensator[18-19] or a fuzzy controller block. However an electrical torque in phase with the speed deviation is to be produced in order to improve damping of the system oscillation. The transfer function block diagram of the damping controller is shown in Fig. 7. It comprises gain block, signal-washout block and lead-lag compensator.
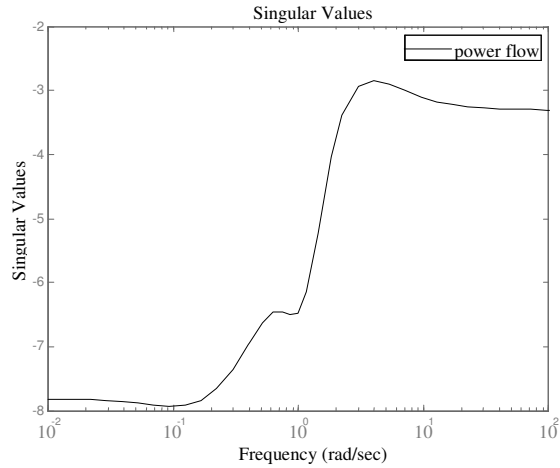

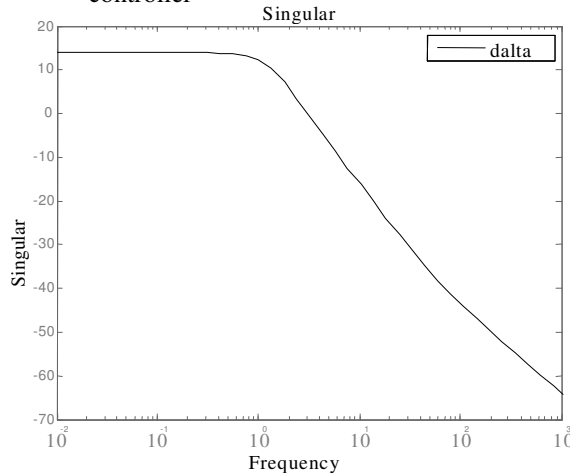Fig. 8: Singular values of open loop of Power flow controller

Fig. 9: Singular values of open loop of DC voltage regulator

CONTROLLER DESIGN USING H$_\infty$ THEORY

Due to system parameters are given in Appendix, the initial d-q axes voltage, current components and torque angle are computed for the nominal operating condition as follows:

$$E_d = 0.396 \text{ pu}; E_q = 0.953 \text{ pu}$$
$$V_E = 1.0233\angle 26.9° \text{ pu}; V_B = 0.1047\angle -55.87° \text{ pu}$$
$$I_d = 0.4317 \text{ pu}; I_q = 0.6601 \text{ pu}; \delta = 51.61°$$

Design of UPFC controller: The UPFC power-flow and DC voltage regulator are designed independently. Based on the procedures explained in section 4, the following controller design results are obtained. First, the singular values of the open loop are calculated and

plotted in Fig. 8. After trial and error, W1 and W2 for power flow controller are chosen:

$$W1 = 15.5 \frac{S + 0.61}{S(S^2 + 11.8S + 18)} \qquad W2 = 1$$

For DC voltage regulator, the same procedure is followed. The singular values of the open loop are calculated and plotted in Fig. 9. W1 and W2 for DC voltage regulator are chosen:

$$W1 = \frac{15(S + 2)}{S(S + 5)} \qquad W2 = 1$$

The variable (γ_{min}) is the inverse of the magnitude of coprime uncertainty, which can be tolerated before getting instability. $\gamma_{min} > 1$ should be as small as possible, and usually requires that γ_{min} is less than a value of $4^{[16-17]}$. By applying this, $\gamma_{min} = 1.3104$ for power flow controller and $\gamma_{min} = 1.3236$ for the DC voltage regulator are obtained. In order to show influence of H_∞ loop-shaping method, the proposed method is compared to conventional method. In conventional method, the parameters of the power-flow controller (k_{pp} and k_{pi}) are optimized using genetic algorithm[20]. Optimum values of the proportional and integral gain settings of the power-flow controller are obtained as $k_{pp} = 2$ and $k_{pi} = 0.35$.

The parameters of DC voltage regulator are now optimized using genetic algorithm. When the parameters of power-flow controller are set at their optimum values. The optimum gain setting of P-I type DC voltage regulator are $k_{dp} = 0.25$ and $k_{di} = 0.35$.

Using a commercially available software package[21], two controllers satisfying design objectives are obtained. For easy implementation, the order has been reduced by model reduction technique. The transfer functions of the controllers are:

$$K_{PF} = \frac{-0.01917S^5 + 20.44S^4 + 27.43S^3 + 35.6S^2 + 11.43S + 0.9874}{S^6 + 16.42S^5 + 18.69S^4 + 24.61S^3 + 7.367S^2 + 0.6474S}$$

$$K_{VDC} = \frac{8.406S^4 + 165.8S^3 + 355.6S^2 + 373S + 125.1}{0.0001S^5 + 0.417S^4 + 20.55S^3 + 159.8S^2 + 91.48S}$$

Design of PSS: The damping controllers are designed to produce an electrical torque in phase with the speed deviation according to phase compensation method. The four control parameters of the UPFC (m_B, m_E, δ_B and δ_E) can be modulated in order to produce the damping torque. In this paper m_B is modulated in order to damping controller design. The speed deviation $\Delta\omega$ is considered as the input to the damping controllers. The

structure of UPFC based damping controller is shown in Fig. 7. It consists of gain, signal washout and phase compensator blocks. The parameters of the damping controller are obtained using the phase compensation technique. The detailed Step-by-step procedure for computing the parameters of the damping controllers using phase compensation technique is given[16, 17]. Damping controller m_B was designed and obtained as follows (wash-out block is considered). Power flow controller damping with damping ratio of 0.5,

$$\text{damping controller} = \frac{536.0145 \quad s \quad (s + 3.656)}{(s + 0.1) \quad (s + 4.5)}$$

RESULTS AND DISCUSSION

In order to examine the robustness of the UPFC power-flow and DC voltage regulator controller in the presence of wide variation in loading condition (three cases), the system load is varied over a wide range. Dynamic responses are obtained for the following three typical loading conditions for $\Delta P_{eref} = 0.1pu$ and $\Delta T_m = 0.1pu$

Case a: P = 0.80pu, Q = 015 pu (nominal load)
Case b: P = 1.00 pu, Q = 0.2 pu (heavy load)
Case c: P = 1.12 pu, Q = 0.285 pu (very heavy load)

The performance of the designed H_∞-UPFC and classic-UPFC controllers with damping controller m_B after sudden change in reference power on transmission line 2, reference mechanical power and reference voltage are shown in Figs. 10 to 15. It can be observed from these figures, which the proposed controller designed (H_∞-UPFC) significantly damp power system oscillations compared to conventional (classical P-I) UPFC controllers (C-UPFC).

In order to investigate the performance of the proposed controller and the system behavior under large disturbances and various operating conditions, a transitory 3-phase fault of 5-10 ms duration at the generator terminals is considered. Dynamic performance is obtained using the non-linear model under the system of the nominal and heavy loading condition with H_∞-based and optimal settings of the UPFC controllers (Power-flow controller, DC-voltage regulator and damping controller). Figure 16 shows the power system responses under the above operation condition. It can be observed from this figure, which the proposed controller designed significantly damp power system oscillations compared to conventional (classical P-I) UPFC controllers (C-UPFC).
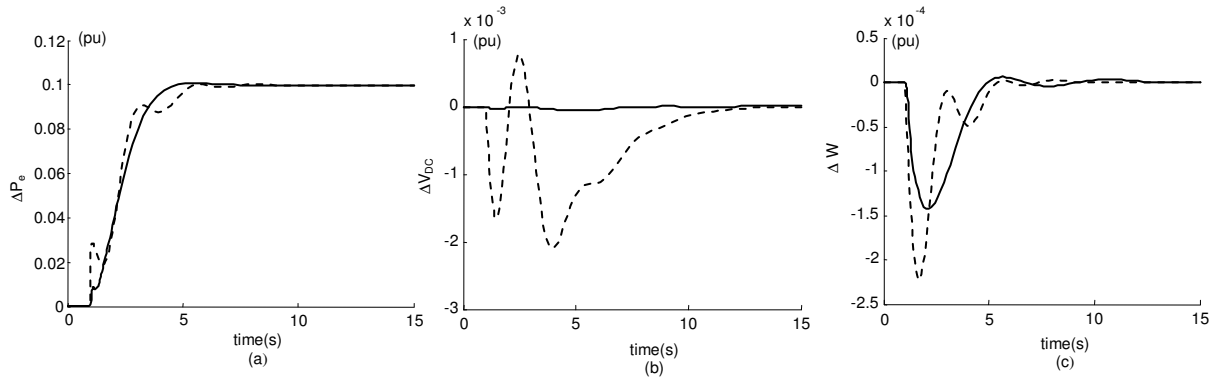
Fig. 10: Dynamic responses at operating point 1 (Nominal loading) during step change in $\Delta P_{e2ref} = 0.1$ pu; Solid (H_∞) and Dashed (Classical a) Power flow deviation on line 2 b) DC- voltage deviation c) Speed deviation
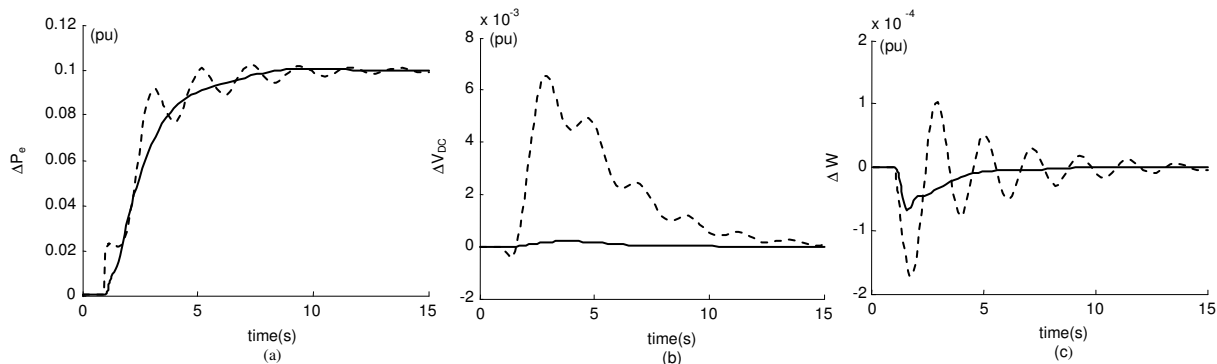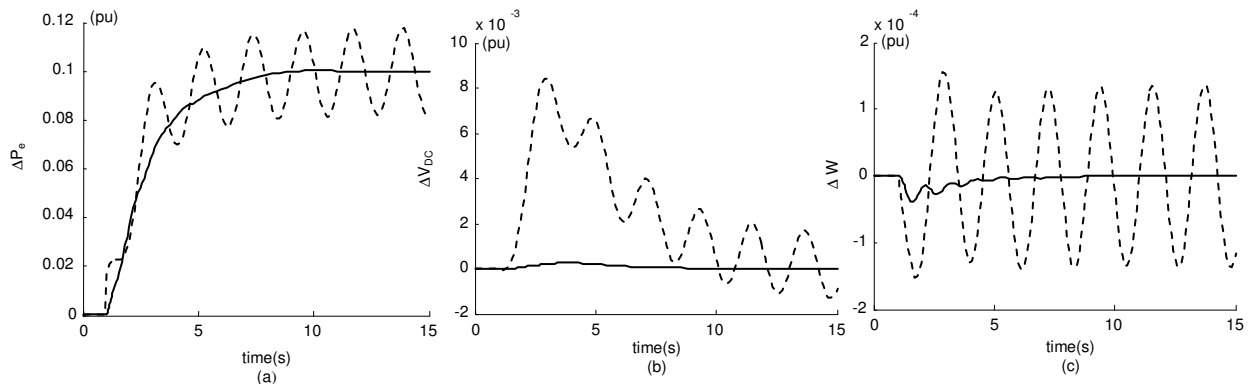

Fig. 11: Dynamic responses at operating point 2 (Heavy loading) during step change in $\Delta P_{e2ref} = 0.1$ pu; Solid (H_∞) and Dashed (Classical) a) Power flow deviation on line 2 b) DC- voltage deviation c) Speed deviation

Fig. 12: Dynamic responses at operating point 3 (Very heavy loading) during step change in $\Delta P_{e2ref}=0.1$ pu; Solid (H_∞) and Dashed (Classical a) Power flow deviation on line2 b) DC- voltage deviation c) Speed deviation

CONCLUSION

In this paper, the design of robust controller based on H_∞ theory with application to an UPFC has been carried out for power system. The performance of the controller has been evaluated in comparison with conventional UPFC by linear and nonlinear time domain simulations. The following issues have been addressed:

• representation of non-linear characteristics of the system by uncertainty model principle.
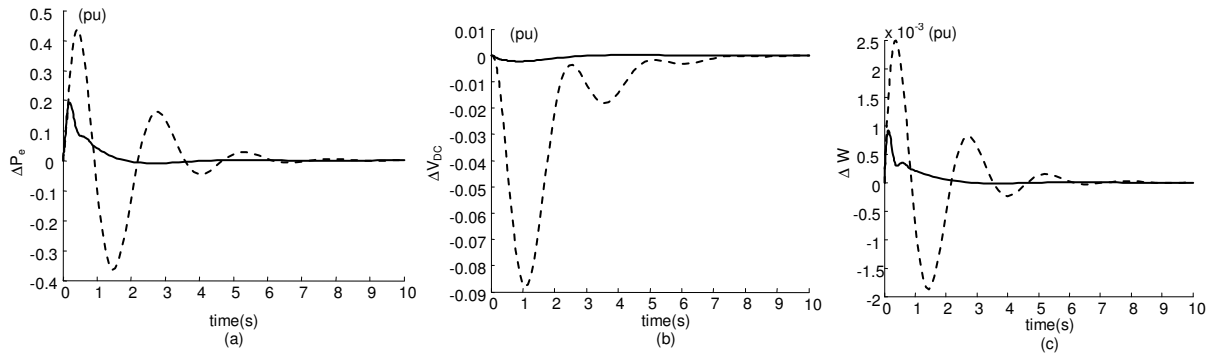
986

Fig. 13: Dynamic responses at operating point 1 (Nominal loading) during step change in ΔT_m=0.1 pu; Solid (H_∞) and Dashed (Classical a) Power flow deviation on line 2 b) DC- voltage deviation c) Speed deviation
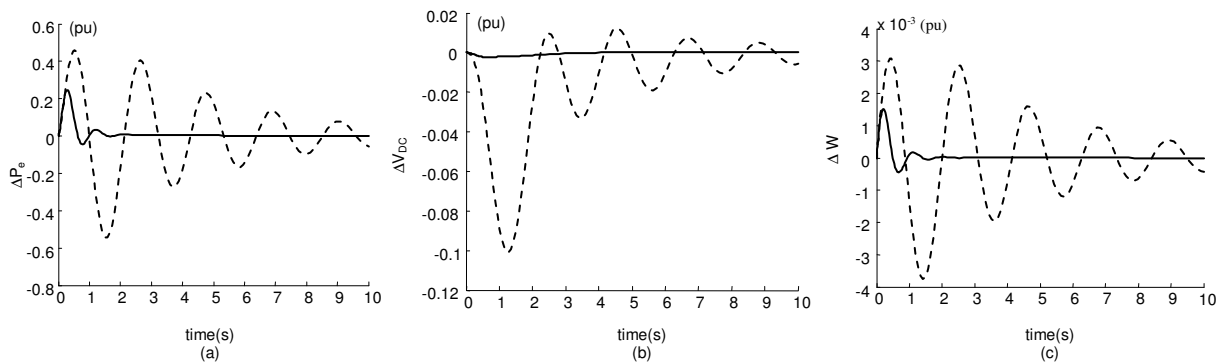

Fig. 14: Dynamic responses at operating point 2 (Heavy loading) during step change in ΔT_m=0.1 pu; Solid (H_∞) and Dashed (Classical a) Power flow deviation on line 2 b) DC- voltage deviation   c) Speed deviation
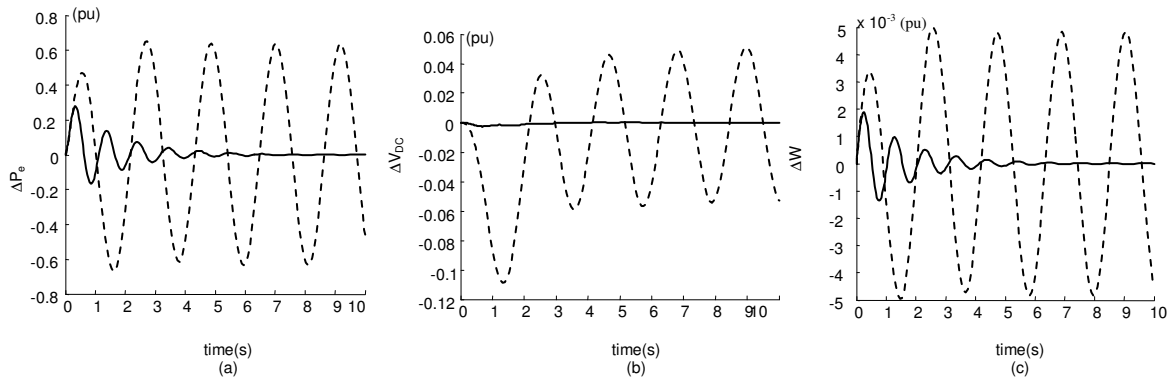

Fig. 15: Dynamic responses at operating point 3 (Very heavy loading) during step change in ΔT_m=0.1 pu; Solid (H_∞) and Dashed (Classical a) Power flow deviation on line 2 b) DC- voltage deviation c) Speed deviation

- selection of appropriate weighting functions based on the control system objectives, and:
- verification of the H_∞ controller design by time domain simulations under various operating conditions.

The main conclusions are:

- The robust controller can improve the damping of power system oscillation.

- The non-linear characteristics of the system can easily by incorporated into the controller design by suitable selection of weighting functions.
- The results of these studies show that the proposed controller design using H_∞ method compared to conventional method, has an excellent capability in damping of power system oscillations.
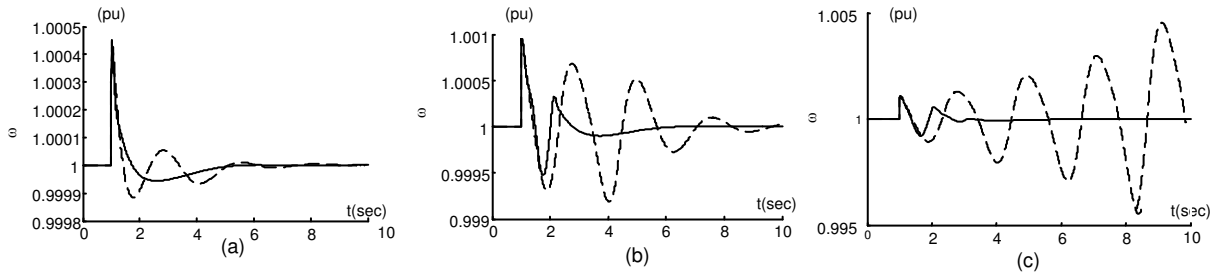
Fig. 16: Speed deviation for a transitory 3-phase fault at the generator terminals, Solid (H_∞-based) and Dashed (Classical) a) For 5ms duration at operating point 1   b) For 10ms duration at operating point 1
c) For 10ms duration at operating point 2

- Performance of damping controllers under large perturbations show the superiority of proposed H_∞-based controller over its conventional counterpart. Also, effectiveness of the proposed control strategy in damping the local low frequency oscillations with UPFC is confirmed.

APPENDIX

The nominal parameters and operating condition of the system are given below:

Generator	$M = 8$ MJ/M	$T'_{do} = 5.044$ sec	$S_d = 1pu$
	$X_q = 0.6$ P.U	$X'_d = 0.3$ pu	$D = 0$
Excitation system	$K_\alpha = 10$	$T_\alpha = 0.05$ sec	
Transformers	$X_{tE} = 0.1$ pu	$X_E = 0.1$ pu	
	$X_B = 0.1$ pu		
Transmission line	$X_{T1} = 1pu$	$X_{T2} = 1.3$ pu	
Operating condition	$P = 0.8pu$	$Q = 0.15pu$	
	$V_t = 1.032$ pu		
DC link parameter	$V_{DC} = 2pu$	$C_{DC} = 3pu$	
UPFC parameter	$m_B = 0.104$	$\delta_B = -55.87$	
	$\delta_E = 26.9°$	$m_E = 1.0233$	

REFERENCES

1. Hingorani N.G. and L. Gyugui, 2000. Understanding FACTS, IEEE Press, New York.
2. Gyugyi L. and C.D. Schauder, 1995. The unified power flow controller: a new approach to power transmission control, ieee trans. pwrd, 10(2): 1085-1093.
3. Gyugyi L., 1992, Unified power flow control concept for flexible ac transmission systems, iee proceedings-c, 139(4): 323-331.
2. Al-Awami A.T., Y.L. Abdel-Magid and M.A. Abido, 2007. A Particle-Swarm-Based Approach of Power System Stability Enhancement with UPFC, Elec. Power and Energy Systems, 29: 251-259.
3. Liou K.L. and Y.Y. Hsu, 1986. Damping of generator oscillation using svc, ieee trans. aero. electron. sys., 22(5): 605-617.
6. Liou K.L. and Y.Y. Hsu, 1992. Damping of generator oscillation using an adaptive static var compensator, ieee trans. pwrs, 7(2): 718-725.
7. Smith J.R., D.A. Pierre, A.D. Rudberg, I. Sadighi and A.P. Johnson, 1989. an enhanced lq adaptive var unit controller for power system damping, ieee trans. PWRS, 4(2): 443-451.
8. Ni Y., L. Jiao, S. Chen and B. Zhang, 1998. Application of a nonlinear pid controller on statcom with a differential tracker, international conference on energy management and power delivery, empd-98, New York: 29-34.
9. Zhao Q., J. Jiang, 1995. Robust SVC Controller Design for Improving Power System Damping, IEEE TPWRS, 10(4): 1927-1932.
10. Parniani M., M.R. Iravani, 1998. Optimal Robust Control Design of SVC, IEE Proc.-C, 125(3): 301-307.
11. Farsangi M.M., Y.H. Song, Y.Z. Sun, 2000. supplementary control design of svc and statcom using H_∞ optimal robust control, international conference electric utility deregulation and restructuring and power technologies, drpt 2000, city university london, uk. pp: 355-360.
12. Farsangi M.M., Y.H. Song, W.L. Fang and X.F. Wang, 2002. Robust FACTS Control Design Using the H_∞ Loop-Shaping Method, IEE Proc.-C, 149(3): 352-358.
13. Nabavi A., M.R. Iravani, 1996. Steady-state and dynamic models of UPFC for power sys. studies, IEEE Trans. PWRS, 11(4): 1937-43.
14. Wang H.F., 1999. Damping function of UPFC, IEE Proc.-C, Vol. 146, No. 1: 81-87.
14. Wang H.F., 1999. Application of modeling UPFC into multi-machine power systems, IEE Proc.-C, 146(3): 306-312.

16. Skogestad S. and I. Postlethwaite, 1996. Multivariable Feedback Control, John Wiley.
17. Zhou K., J.C. Doyle, K. Glover, 1996. Robust and Optimal Control, Prentice-Hall, Inc.
18. YU Y.N., 1983. Electric Power System Dynamics, Academic Press, Inc., London.
19. Eldamaty A.A., S.O. Faried, S. Aboreshaid, 2005. Damping PSO Using a Fuzzy Logic Based UPFC, IEEE CCECE/CCGEI, 1: 1950-1953.
20. Randy L.H., E.H. Sue, 2004. Practical Genetic Algorithms, John Wiley & Sons, Second Edition. MATLAB Software, The Mathworks, Inc. 2006.